Relativistic effects in plasma produced with sub-nanosecond 3-TW laser

J. Krása[1], D. Klír[2,3], K. Řezáč[2,3], J. Cikhardt[2,3], M. Krůs[3,1], A. Velyhan[1], M. Pfeifer[1,3],
J. Dostál[3,1], R. Dudžák[1,3], M. Krupka[3], J. Kaufman[1],
T. Pisarczyk[4], Z. Kalinowska[4], T. Chodukowski[4]

[1] *Institute of Physics of the Czech Academy of Sciences, Prague, Czech Republic*
[2] *Faculty of Electrical Engineering, Czech Technical University in Prague, Czech Republic*
[3] *Institute of Plasma Physics of the Czech Academy of Sciences, Prague, Czech Republic*
[4] *Institute of Plasma Physics and Laser Microfusion, Warsaw, Poland*

Abstract — This contribution deals with observations of relativistic electrons produced in a laser plasma interaction experiment at the PALS laser system operated at the Institute of Plasma Physics in Prague. The PALS laser is a near-infrared 3-TW iodine laser designed to deliver irradiance on target of 10^{16} $\mathrm{Wcm^{-2}}$ in ≈300 ps pulses at the wavelength of 1.315 μm. Various foils of 6 – 500 μm in thickness were irradiated with $I\lambda^2 \approx 5\times10^{16}$ W $\mathrm{cm^{-2}}$ $\mathrm{\mu m^2}$. Under these conditions we have observed relativistic electrons expanding into the vacuum with maximum energy going beyond 4 MeV. The relativistically accelerated forward electrons escaping from the rear target surface were observed with the use of electron energy analysers. The observed electron energy spectra indicate that the applied laser intensity was increased by the thermal and relativistic self-focusing. The application of a unique femtosecond interferometry technique allowed us to observe bunches of thermal electrons occurring in the plasma expanding against the focused laser beam.

The prima facie evidence of the relativistic electrons produced at the intensity of $I\lambda^2 \sim 5\times10^{16}$ $\mathrm{Wcm^{-2}\mu m^2}$ delivered by the PALS laser system has been presented in [1]. The production of MeV-protons and highly charged heavy ions at this intensity has been ascribed to the self-focusing and proved experimentally [2]. In general terms, solving the problem of propagation of the laser pulse of $I > 10^{14}$ $\mathrm{W/cm^2}$ through a plasma has led to the discovery of thermal, relativistic, and ponderomotive self-focusing [3-6]. The analysis of PALS experimental conditions shows that only two of the mentioned non-linear processes can occur during the laser-matter interaction: the thermal and relativistic self-focusing.

When the electron oscillation becomes relativistic the ponderomotive acceleration of electrons establishes the temperature of hot electrons [7]:

$$T_h = 0.511 \cdot \left(\sqrt{1 + \frac{I\lambda^2[\mathrm{Wcm^{-2}\mu m^2}]}{1.37\times10^{18}}} - 1 \right) \mathrm{MeV}. \quad (1)$$

This relationship gives $T_h \approx 9$ keV for the applied $I\lambda^2 \sim 5\times10^{16}$ Wcm^{-2}μm^2. However, the electron energy spectrum obtained with the use of magnetic dipole spectrometers equipped with a pair of magnets producing a uniform magnetic field equal to 160 mT and electron sensitive image plate, has a peak at 420 keV and decreases exponentially with T ≅ 655 keV, as Fig. 1 shows.

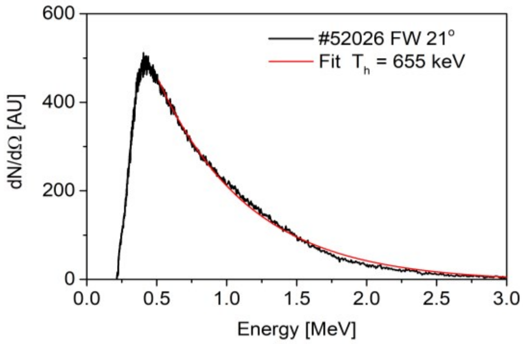

Fig. 1 Electron energy distribution observed in the forward direction $\phi_{FW} = 21°$ and fit of exp(-E/T) function to experimental data. The electrons were emitted from a 500-μm thick deuterated polyethylene foil irradiated by the 3TW laser delivering an intensity of 5×10^{16} Wcm^{-2}μm^2 in 350 ps.

According to equation (1) the fitted value $T_h \cong 655$ keV corresponds to the value of laser intensity $I\lambda^2 \sim 6\times10^{18}$ Wcm^{-2}μm^2. This value can be reached only when the focal spot of the laser beam is shrink at least by a factor of ≅ 11 to the diameter of 5 -7 μm. This should be the result of self-focusing. It is evident that the self-focusing starts at the beginning of the laser-target interaction. The intensity threshold for the classical thermal filamentation, I_{TF}, has been given by W. L. Kruer [8] who estimated:

$$I_{TF}\lambda \geq 2 \times 10^{15} \frac{n_c}{n_e}\frac{T_e}{L} \ , \quad (2)$$

where the threshold intensity I_{TF} is in W/cm^2 units, λ is the laser wavelength in μm units, T_e is the electron temperature in keV units, L is the scale plasma length $L = n_e/\ (\partial n_e/\partial z)$ in μm units, and $n_c = 6.5\times10^{20}$ cm^{-3} for the 1.315-μm iodine laser. The basic value of $I = 2\times10^{15}$ Wcm^{-2} in (2) is reached ≈ 300 ps before the maximum laser intensity of 5×10^{16} Wcm^{-2}μm^2 irradiates the target. As (2) estimates for values $L \approx 100$ μm and $n_e \approx 1\times10^{20}$ cm^{-3} taken from the corresponding PALS data [9], the thermal self-focusing can happen when $T_e \leq$ 20 keV. This condition can be fulfilled because numerical modeling gives T_e <3 keV and experimental observations confirm this. [9]. We can conclude that thermal filamentation (or self-focusing) takes place under our experimental conditions. This process leads to the gradual increase in the focused intensity, and can lead to the formation or alteration of other instabilities, to change the location of energy deposition, and possibly to cause collective effects such as the generation of hot electrons [8]. This also leads to time-space variations in the electron density, as Fig. 2 shows. The electron density, which was calculated from femtosecond interferograms, varies significantly during the laser-plasma interaction [9,10]. The shown chain of islands in the electron density represents the very complex structure of electron bunches which was observed at the end of the laser-plasma interaction. These bunches contain only thermal plasma electrons expanding into the vacuum with low velocity of about 7×10^5 m/s [10]. The structure of the electron density distribution suggests that that both fast ions and hot electrons can be emitted in bursts that arise in different places and times [10]. It is obvious that at the time of obtaining the interferogram data, which have been transformed to Fig. 2, the relativistic electrons are already a few dozen centimeters away from the target.

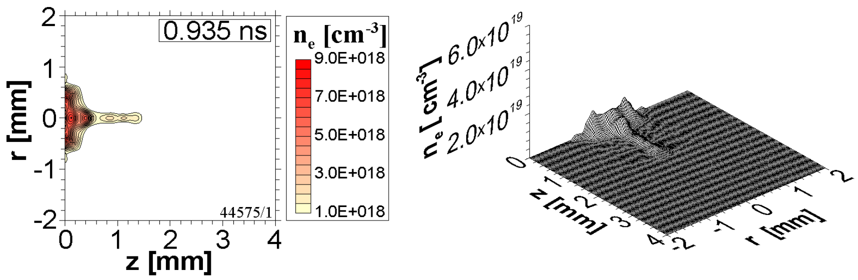

Fig. 2 Electron density distribution observed in the backward direction observed at 0.935 ns after the maximum of laser intensity. The electrons were emitted from a 6 μm thin niobium foil irradiated by the PALS laser delivering an intensity of about 5×10^{16} Wcm^{-2}μm^2 onto the target in 350 ps.

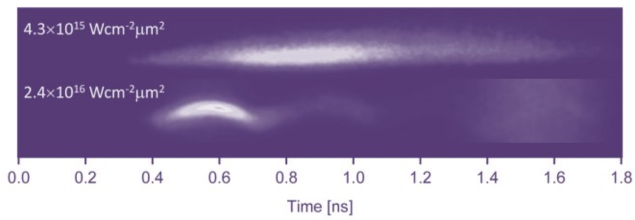

Fig. 3 Time-space diagrams of X-ray emission by deuterated polyethylene plasma at the front side of the target exposed to various laser intensity, as labels show. Streaks were obtained with the use of an X-ray streak camera placed in a side view of the target. The entrance slit parallel to the target surface allows imagining the plasma with spatial resolution of 25 μm along the target normal. The X-ray radiation with the photon energy $E_{ph} > 0.8$ keV is integrated over the target cross section

The occurrence of the self-focusing is also followed by disturbances in the X-ray emission from the thermal plasma, as the time-space visualization of the corona displacement on the micrometre scale in the vicinity of the target surface shows, see Fig. 3. When the laser intensity is low $I\lambda^2 = 2.5\times10^{15}$ Wcm^{-2}μm^2, then the corona displacement is very low: $v \approx 5\times10^4$ m/s. The increase in the intensity to 2.4×10^{16} Wcm^{-2}μm^2 leads not only to the increase in the displacement velocity but also to the undulation of the time-space track, for which a backward shift is characteristic. This shift could be caused by the self-focusing pushing the critical density upstream the laser beam. The increasing laser intensity leads to decrease in the undulation period and causes a collapse in the soft X-ray emission. The intensively radiating part of the corona loses its character of a point-like soft X-ray source. We note that besides the classical thermal filamentation, the relativistic self-focusing can occur because the relativistic threshold of ≈ 1 TW is reachable when the whole laser beam interacts with the underdense region where $n_e > 1\times10^{19}$ cm^{-3} [12].

In conclusion, the emission of relativistic electrons as well as MeV protons by the plasma produced with the use of the 3-TW PALS laser is caused by the laser beam self-focusing. In addition to thermokinetic forces, nonlinear forces become dominant in electron and ion acceleration at irradiance of 10^{16} Wcm^{-2}μm^2.

Acknowledgments

The research leading to these results has received funding from the Czech Science Foundation (Grant No. 16-07036S), CTU grant No. SGS16/223/OHK3/3T/13, the Czech Republic's Ministry of Education, Youth and Sports (project LM2015083, OPVVV project Creating and probing dense plasmas CZ.02.1.01/0.0/0.0/16_013/0001552, and ADONIS project Advanced research using high intensity laser produced photons and particles CZ.02.1.01/0.0/0.0/16_019/0000789).

References

[1] S. Singh et al. 43rd EPS Conference on Plasma Physics, Leuven, Belgium 2016, Europhysics Conference Abstracts, Vol. 40A, ISBN: 2-914771-99-1, P2.102.
[2] L. Láska et al. Laser Part. Beams **24**, 175 (2006).
[3] R. S. Craxton, and R. L. McCrory. J. Appl. Phys. **56**, 108 (1984).
[4] G.-Z. Sun, E. Ott, Y.C. Lee, P. Guzdar. Phys. Fluids **30**, 526 (1987).
[5] W. B. Mori et al. Phys. Rev. Lett. **60**, 1298 (1988).
[6] R. S. Craxton et al. Phys. Plasmas **22**, 110501 (2015).
[7] S. C. Wilks, W. L. Kruer, M. Tabak, and A. B. Langdon, Phys. Rev. Lett. **69**, 1383 (1992).
[8] W.L. Kruer, In: Laser program annual report 1984. Rufer, M.L.; Murphy, P.W. (eds.); Lawrence Livermore National Lab., CA (USA); p. 3.32-3.35; Jun 1985; p. 3.32-3.35.
[9] T. Pisarczyk, et al., Phys. Plasmas **21**, 012708 (2014).
[10] T. Pisarczyk, et al., Laser Part. Beams **33**, 221 (2015).
[11] J. Krasa et al. Laser Part. Beams **27**, 171 (2009).
[12] P. Mulser, D. Bauer. In: High Power Laser-Matter Interaction. Springer Tracts in Modern Physics, Vol. 238. (Springer Berlin Heidelberg, 2010), ISBN 3540506691, 9783540506690. p. 400.